# Carboxy and Diphosphate Ester Hydrolysis by a Dizinc Complex with a New Alcohol-Pendant Macrocycle

**Carla Bazzicalupi,[†] Andrea Bencini,*[,†] Emanuela Berni,[†] Antonio Bianchi,*[,†] Valentina Fedi,[†] Vieri Fusi,[‡] Claudia Giorgi,[†] Piero Paoletti,*[,†] and Barbara Valtancoli[†]**

Department of Chemistry, University of Florence, Via Maragliano 75/77, 50144 Florence, Italy, and Institute of Chemical Sciences, University of Urbino, Urbino, Italy

*Received March 16, 1999*

The synthesis of the new alcohol-pendant macrocycle 4-(2-hydroxyethyl)-1,4,7,16,19,22-hexaaza-10,13,25,28-tetraoxacyclotriacontane (**L2**) is reported. This ligand contains two different triamine moieties, one of them bearing an ethanolic sidearm. **L2** binds two Zn(II) ions in aqueous solution. The stability constants of the **L2** complexes have been determined at 298.1 and 308.1 K by means of potentiometric measurements. Besides a $[Zn_2\mathbf{L2}]^{4+}$ species, a deprotonated $[Zn_2(\mathbf{L2}\text{-H})]^{3+}$ complex and a hydroxo $[Zn_2(\mathbf{L2}\text{-H})(OH)]^{2+}$ complex are formed in aqueous solution. Zn(II)-assisted deprotonation of the alcoholic group takes place at neutral pH, giving the $[Zn_2(\mathbf{L2}\text{-H})]^{3+}$ complex. In $[Zn_2(\mathbf{L2}\text{-H})]^{3+}$, the deprotonated R−O$^-$ function bridges the two metals, as shown by the crystal structure of $[Zn_2(\mathbf{L2}\text{-H})Br_2]BPh_4\cdot$MeOH. The hydroxo species $[Zn_2(\mathbf{L2}\text{-H})(OH)]^{2+}$ is formed at slightly alkaline pH's. This complex contains both a Zn(II)-bound alkoxide and a Zn(II)−OH nucleophilic function. Therefore, it may provide a simple model system for alkaline phosphatases, where both a deprotonated serine and a Zn−OH function are involved in phosphate ester hydrolysis. Indeed, this complex promotes the hydrolysis of the carboxy ester *p*-nitrophenyl acetate (NA) as well as the cleavage of phosphate ester bis(*p*-nitrophenyl) phosphate (BNP). The kinetics of promoted hydrolysis of NA and BNP were studied by means of UV and $^1$H and $^{31}$P NMR measurements. In NA hydrolysis, the R−O$^-$−Zn(II) function acts as nucleophile in the first step of the hydrolytic mechanism, to give an acetyl derivative, which is subsequently hydrolyzed to acetate by a Zn−OH group. Similarly, in BNP cleavage, the nucleophilic attack of alkoxide on phosphorus gives a pendant-alcohol phosphorylated intermediate, which undergoes subsequent intramolecular nucleophilic attack of a Zn(II)-bound hydroxide to yield a phosphomonoester product.

## Introduction

A number of zinc enzymes with multinuclear metal sites are known to be responsible for the hydrolysis of the phosphate ester bond in a variety of low molecular weight metabolites and nucleic acids.[1−14] In particular, alkaline phosphatase (AP) contains two Zn(II) ions with different coordination environments (ca. 4 Å separation).[10−13] This enzyme hydrolyzes phosphate monoesters by using the two cooperative Zn(II) ions at the active center. On the other hand, a serine (102) group is involved in the hydrolytic mechanism. It is now considered that the phosphate ester, coordinated by the Zn(II) ions, is initially attacked by the deprotonated serine to give a phosphoserine intermediate, which is subsequently attacked by an adjacent Zn−OH function to complete the hydrolytic process and reproduce the free form of serine. (See Scheme 1.)

Several synthetic Zn(II) complexes have been used as model systems for this enzyme.[15−37] Zn(II) macrocyclic triamine and tetraamine complexes with an alkoxide pendant (such as **1** and

[†] University of Florence.
[‡] University of Urbino.

(1) Sigel H., Ed. *Zinc and its Role in Biology and Nutrition*; Marcel Dekker: New York, 1983.
(2) Bertini, I., Luchinat, C., Marek, W.; Zeppezauer, M., Eds. *Zinc Enzymes*, Birkauser: Boston, MA, 1986.
(3) Kim, E. E.; Wyckoff, H. W. *J. Mol. Biol.* **1991**, *218*, 449−464.
(4) Coleman, J. E. *Annu. Rev. Biophys. Biomol. Struct.* **1992**, *21*, 441−483.
(5) Gani, D.; Wilkie, J. *Chem. Soc. Rev.* **1995**, 55−63.
(6) Lipscomb, W. N.; Sträter N. *Chem. Rev.*, **1996**, *96*, 2375−2434.
(7) Wilcox, D. E. *Chem. Rev.* **1996**, *96*, 2435−2458.
(8) Steinhagen, H.; Helmchen, G. *Angew. Chem., Int. Ed. Engl.* **1996**, *35*, 2339−2342.
(9) Sträter, N.; Lipscomb, W. N.; Klabunde, T.; Krebs, B. *Angew. Chem., Int. Ed. Engl.* **1996**, *35*, 2024−2055.
(10) Gettins, P.; Coleman, J. E. *J. Biol. Chem.* **1994**, *259*, 4991−4997.
(11) Ma, L.; Tibbitts, T. T.; Kantrovitz, E. R. *Protein Sci.* **1995**, *4*, 1498−1506.
(12) Hollfelder, F.; Herschlag, D. *Biochemistry* **1995**, *34*, 12255−12264.
(13) Murphy, J. E.; Tibbits, T. T.; Kantrovitz, E. R. *J. Mol. Biol.* **1995**, *253*, 604−617.
(14) Hough, E.; Hansen, L. K.; Birknes, B.; Jynge, K.; Hansen, S.; Hardvik, A.; Little, C.; Dodson, E.; Derewenda, Z. *Nature* **1989**, *338*, 357−358.
(15) Gellman, S. H.; Petter, R.; Breslow, R. *J. Am. Chem. Soc.* **1986**, *108*, 2388−2394.
(16) Chapman, W. H., Jr.; Breslow, R. *J. Am. Chem. Soc.* **1995**, *117*, 5462−5469.
(17) Koike, T.; Kimura, E. *J. Am. Chem. Soc.* **1991**, *113*, 8935−8941.
(18) Koike, T.; Kimura, E.; Nakamura, I.; Hashimoto, Y.; Shiro, M. *J. Am. Chem. Soc.* **1992**, *114*, 7338−7345.
(19) Kimura, E. *Tetrahedron* **1992**, *30*, 6175−6217.
(20) Looney, A.; Parkin, G.; Alsfasser, R.; Ruf, M.; Vahrenkamp, H. *Angew. Chem., Int. Ed. Engl.* **1992**, *31*, 92−93.
(21) Alsfasser, R.; Ruf, M.; Trofimenko, S.; Vahrenkamp, H. *Chem. Ber.* **1993**, *126*, 703−710.
(22) Ruf, M.; Weis, K.; Vahrenkamp, H. *J. Chem. Soc., Chem. Commun.* **1994**, 135−136.
(23) Ruf, M.; Weis, K.; Vahrenkamp, H. *J. Am. Chem. Soc.* **1996**, *118*, 9288−9294.
(24) Hikichi, S.; Tanaka, M.; Moro-oka, Y.; Kitajima, N. *J. Chem. Soc., Chem. Commun.* **1992**, 814−815.
(25) Garcia-España, E.; Luis, S. *Supramol. Chem.* **1996**, *6*, 257−266.
(26) Altava, B.; Burguete, M. I.; Luis, S. V.; Miravet, J. F.; Garcia-España, E.; Marcelino, V.; Soriano, C. *Tetrahedron*, **1997**, *57*, 4751−4762.

10.1021/ic9902929 CCC: $18.00 
Published on Web 08/20/1999

**Scheme 1**

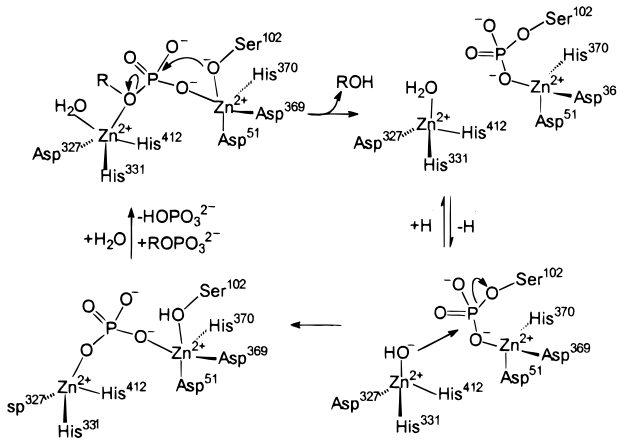

**Chart 1**

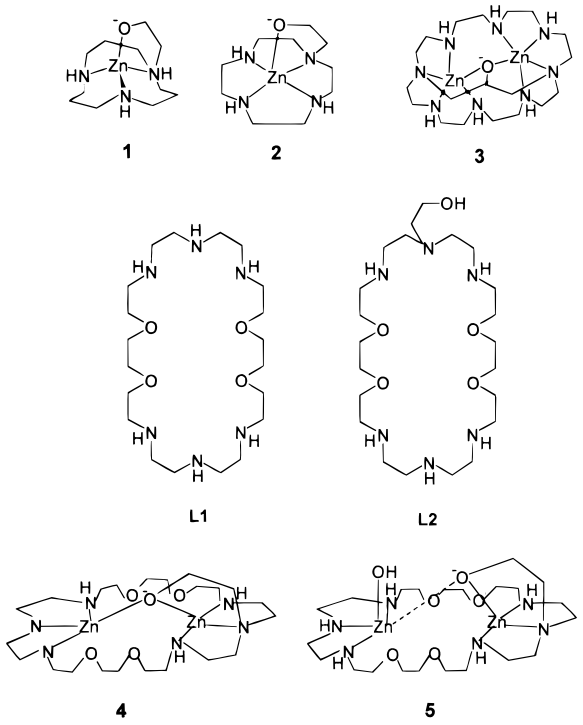

**2** in Chart 1) were recently studied by Kimura and co-workers, to elucidate the role of the alcohol pendant in the hydrolysis of carboxy and diphosphate esters.[28−31] It was found that Zn(II)-assisted deprotonation of the alcohol pendant gives a $RO^-$−Zn(II) function, which is a better nucleophile than a Zn−OH function. The selective recognition and hydrolysis of activated phosphate monoesters were successfully achieved by the same authors using a dinuclear Zn(II) complex with a propanol-bridged octaazacryptand (**3** in Chart 1).[32] In this case, however, the nuclephilic attack on the substrate is given by an amine group weakly bound to the metal.

Recently we reported that the Zn(II) binuclear complex with ligand **L1** is able to promote the hydrolysis of activated phosphate diesters.[33,34] The two Zn(II) ions work cooperatively in the hydrolytic mechanism, through a bridging interaction of the phosphate substrate with the two metals and a simultaneous nucleophilic attack of a Zn−OH function on the substrate.

To combine the enhanced binding interaction with phosphate substrates of a dinuclear core having the special nucleophilic properties of a Zn(II)-coordinated alkoxide pendant, we have strategically appended an alcohol pendant to macrocycle **L1**. It is expected that the resulting macrocycle **L2** can give binuclear Zn(II) complexes in which the two metals are kept at close distance by the macrocyclic framework. We hoped that the pendant alcohol could be deprotonated upon Zn(II) coordination, giving a strongly nucleophilic R−$O^-$ function, able to act as catalytic site in a fashion similar to that of the serine group in alkaline phosphatases. Indeed, we have found that **L2** gives a dinuclear Zn(II) complex containing a deprotonated alcoholic function at neutral pH (**4** in Chart 1). At slightly alkaline pH's, binding of a hydroxide anion leads to the formation of complex **5**, which contains both a Zn(II)−alkoxide and a Zn−hydroxide function at close distance, similar to situation found in alkaline phosphatases.

We herein describe the synthesis and reactivity toward carboxy and phosphate esters of this novel chemical model for Zn(II)-containing serine enzymes.

## Experimental Section

**General Methods.** All reagents and solvents used were of analytical grade. *p*-Nitrophenyl acetate was recrystallized from diethyl ether.

UV spectra were recorded on a Shimadzu UV-2101PC spectrophotometer. The 200.0 MHz $^1$H, 50.32 MHz $^{13}$C NMR, and 81.01 MHz $^{31}$P NMR spectra obtained for $D_2O$ solutions at different pH values were recorded on a Bruker AC-200 spectrometer. $^1$H NMR peak positions are reported relative to HOD at 4.75 ppm. Dioxane was used as the reference standard for $^{13}$C NMR spectra (=67.4 ppm). $^1$H−$^1$H and $^1$H−$^{13}$C 2D correlation experiments were performed to assign the signals. $^{31}$P NMR peak positions are reported relative to an external reference of 85% $H_3PO_4$. In $^1$H and $^{31}$P NMR experiments at different pH's, small amounts of 0.01 mol $dm^{-3}$ NaOD or DCl solutions were added to a solution of the ligand to adjust the pD. The pH was calculated from the measured pD values using the relationship pH = pD − 0.40.[38]

The kinetics of BNP cleavage were followed by means of $^1$H and $^{31}$P NMR spectra recorded at different times for $D_2O$ solutions (pH 10, CAPS buffer, 0.1 mol $dm^{-3}$ $NMe_4NO_3$) containing $[Zn_2(\mathbf{L2}\text{-H})](ClO_4)_3 \cdot 2H_2O$ and BNP (0.02 mol $dm^{-3}$) at 308 K.

**Synthesis of the Compounds.** 1,4,7,16,19,22-Hexaaza-10,13,25,28-tetraoxacyclotriacontane (**L1**) and **6** were prepared as previously described.[33]

**1,7-Bis(*p*-tolylsulfonyl)-4-(2-hydroxyethyl)-1,4,7-triazaheptane (6).** A solution of *N*-(*p*-tolylsulfonyl)aziridine (24.8 g, 0.126 mol) in acetonitrile (400 $cm^3$) was added, over a period of ca. 4 h, to a refluxing solution of ethanolamine (3.6 g, 0.059 mol) in acetonitrile (200 $cm^3$). After 20 min of reflux, the reaction mixture was cooled to room temperature, the resulting suspension was filtered, and the filtrate was evaporated under reduced pressure to give a yellowish oil. Diethyl ether

(27) Ragunathanm, K. G.; Schneider, H.-J. *Angew. Chem., Int. Ed. Engl.* **1996**, *35*, 1219−1220.
(28) Kimura, E.; Nakamura, I.; Koike, T.; Shionoya, M.; Kodama, Y.; Ikeda, T.; Shiro, M. *J. Am. Chem. Soc.* **1994**, *116*, 4764−4771.
(29) Koike, T.; Kajitani, S.; Nakamura, I.; Kimura, E.; Shiro, M. *J. Am. Chem. Soc.* **1995**, *117*, 1210−1219.
(30) Koike, T.; Kimura, E.; Kodama, M.; Shiro, M. *J. Am. Chem. Soc.* **1995**, *117*, 8304−8311.
(31) Kimura, E.; Koike, T. *J. Chem. Soc., Chem. Commun.* **1998**, 1495−1500 and references therein.
(32) Koike, T.; Inoue, M.; Kimura, E.; Shiro, M. *J. Am. Chem. Soc.* **1996**, *118*, 3091−3099.
(33) Bazzicalupi, C.; Bencini, A.; Bianchi, A.; Fusi, V.; Paoletti, P.; Piccardi, G.; Valtancoli, B. *Inorg. Chem.* **1995**, *34*, 5622−5631.
(34) Bazzicalupi, C.; Bencini, A.; Bianchi, A.; Fusi, V.; Giorgi, G.; Paoletti, P.; Valtancoli, B.; Zanchi, D. *Inorg. Chem.* **1997**, *36*, 2784−2790.
(35) Sigel, H. *Coord. Chem. Rev.* **1990**, *100*, 453−489.
(36) Chin, J. *Acc. Chem. Res.* **1991**, *24*, 145−152.
(37) Chadhuri, P.; Atockneim, C.; Wieghardt, K.; Deck, W.; Gregorzic, R.; Vahrenkamp, H.; Nuber, B.; Weiss, J. *Inorg. Chem.* **1992**, *31*, 1451.
(38) Covington, A. K.; Paabo, M.; Robinson, R. A.; Bates, R. G. *Anal. Chem.* **1968**, *40*, 700.

(300 $cm^3$) was then added under magnetic stirring, and the resulting solid was collected and washed with ether. Yield: 19.2 g (71%). Anal. Calcd for $C_{20}H_{29}N_3O_5S_2$: C, 52.73; H, 6.42; N, 9.22. Found: C, 52.87; H, 6.57; N, 9.35.

**1,7,16,19,22-Pentakis(*p*-tolylsulfonyl)-4-(2-hydroxyethyl)-1,4,7,16,19,22-hexaaza-10,13,25,28-tetraoxacyclotriacontane (8).** A solution of sodium (1.26 g, 0.055 mol) in dry ethanol (50 $cm^3$) was added to a suspension of **6** (13.85 g, 0.0304 mol) in dry ethanol (75 $cm^3$). The resulting mixture was refluxed for ca. 30 min, and the solvent was evaporated under reduced pressure. The solid residue was dissolved in dry DMF (800 $cm^3$), and $K_2CO_3$ (60 g, 0.43 mol) was added. To the resulting suspension heated at 115 °C was added **7** (30 g, 0.0304 mol) in dried DMF (1 $dm^3$) over a period of ca. 6 h. The reaction mixture was kept at 115 °C for a further 12 h. After being cooled at room temperature, the suspension was poured into ice-cold water, and the precipitate was decanted and washed with water. The crude product was purified by chromatography on silica gel (230−400 mesh) eluting with chloroform. The eluted fractions were collected and evaporated to dryness to obtain **8** as a white solid. Yield: 4.2 g (11%). Anal. Calcd for $C_{57}H_{80}N_6O_{15}S_5$: C, 54.79; H, 6.46; N, 6.73. Found: C, 54.52; H, 6.59; N, 6.64. $^1$H NMR ($CDCl_3$) (ppm): 2.75 (t, 4H), 3.32 (t, 4H), 3.15 (m, 8H) (N−$CH_2$−$CH_2$−N ethylenic chains), 3.26 (m, 8H) 3.54 (m, 8H) (N−$CH_2$−$CH_2$−O ethylenic chains), 3.44 (m, 8H) (O−$CH_2$−$CH_2$−O), 2.60 (t, 2H), 3.40 (t, 2H) (N−$CH_2$−$CH_2$−OH), 2.36 (s, 6H), 2.38 (s, 6H), 2.40 (s, 3H), 7.23 (d, 4H), 7.27 (d, 4H), 7.30 (d, 2H), 7.64 (d, 2H), 7.67 (d, 4H), 7.70 (d, 4H) (tosyl groups). $^{13}$C NMR ($CDCl_3$) (ppm): 45.9, 49.0, 49.2, 49.3 (N−$CH_2$−$CH_2$−N ethylenic chains), 49.4, 49.8, 70.1, 70.2 (N−$CH_2$−$CH_2$−O), 70.4, 70.6 (O−$CH_2$−$CH_2$−O), 56.7, 59.3, (N−$CH_2$−$CH_2$−OH), 21.5, 127.2, 127.3, 127.5, 129.7, 129.8, 129.9, 135.5, 135.9, 136.6, 143.2, 143.5, 143.7 (tosyl groups).

**4-(2-Hydroxyethyl)-1,4,7,16,19,22-Hexaaza-10,13,25,28-tetraoxacyclotriacontane Hexahydrochloride Dihydrate (L2·6HCl·2$H_2O$).** Onto a suspension of **8** (3.5 g, 2.8 × $10^{-3}$ mol) in diethyl ether (30 $cm^3$) and methanol (1 $cm^3$) cooled at −70 °C was condensed 500 $cm^3$ of ammonia. When small bits of lithium were added (ca. 10 mg each piece), the reaction mixture became blue. The addition was continued until the suspension maintained the blue color for at least 5 min, and then $NH_4Cl$ (12 g, 0.2 mol) was added in small portions. Evaporation of ammonia at room temperature gave a white solid residue, which was treated with 3 M HCl (300 $cm^3$). The resulting suspension was washed with chloroform (3 × 100 $cm^3$), the aqueous layer was filtered, and the filtrate was evaporated to dryness under reduced pressure to give a white solid. This product was dissolved in a minimum amount of water, and the resulting solution was made alkaline with NaOH. This solution was extracted with $CHCl_3$ (6 × 100 $cm^3$). The organic layer was dried over anhydrous $Na_2SO_4$ and evaporated under reduced pressure, affording the macrocycle **L2** as a colorless oil. The hexahydrochloride salt was obtained by adding 37% HCl to an ethanolic solution containing the free amine. The white solid formed was filtered off and washed with ethanol. Yield: 0.3 g (15%). Anal. Calcd for $C_{22}H_{60}N_6O_7Cl_6$: C, 36.03; H, 8.25; N, 11.46. Found: C, 36.18; H, 7.99; N, 11.21. $^1$H NMR ($D_2O$, pH 3) (ppm): 3.26 (t, 4H), 3.40 (t, 4H), 3.55 (m, 8H) (N−$CH_2$−$CH_2$−N ethylenic chains), 3.30 (t, 4H), 3.36 (t, 4H), 3.78 (t, 4H), 3.82 (t, 4H) (N−$CH_2$−$CH_2$−O), 3.72 (m, 8H) (O−$CH_2$−$CH_2$−O), 3.02 (t, 2H), 3.74 (t, 2H) (N−$CH_2$−$CH_2$−OH). $^{13}$C NMR ($D_2O$, pH 3) (ppm): 44.2, 44.7, 44.8, 51.0 (N−$CH_2$−$CH_2$−N ethylenic chains), 66.6, 66.8, 48.7, 49.0 (N−$CH_2$−$CH_2$−O ethylenic chains), 70.8, 71 (O−$CH_2$−$CH_2$−O ethylenic chain), 56.2, 58.7 (N−$CH_2$−$CH_2$−OH).

**[$Zn_2$(L2-H)]$(ClO_4)_3$·2$H_2O$.** A sample of $Zn(ClO_4)_2$·6$H_2O$ (37.3 mg, 0.1 mM) was added to a methanol solution (10 $cm^3$) of **L2** (25 mg, 0.05 mM). Butanol (10 $cm^3$) was then added. Upon slow evaporation of this solution, a colorless powder crystallized, which was filtered off and dried under vacuum. Yield: 39 mg (80%). Anal. Calcd for $C_{22}H_{53}Cl_3N_6O_{19}Zn_2$: C, 28.03; H, 5.67; N, 8.91. Found: C, 28.0; H, 5.8; N, 8.9. *Caution!* Perchlorate salts are potentially explosive; these compounds must be handled with great caution.

**[$Zn_2$(L2-H)$Br_2$]$BPh_4$·MeOH.** NaBr (10 mg 0.1 mM) and $NaBPh_4$ (6.8 mg, 0.02 mmol) were added to a methanolic solution (10 $cm^3$) of [$Zn_2$(**L2**-H)]$(ClO_4)_3$·2$H_2O$ (9.4 mg, 0.01 mmol). Addition of butanol (10 $cm^3$) led to crystallization of the complex. Yield: 10.1 mg (90%). Anal. Calcd for $C_{47}H_{73}BBr_2N_6O_6Zn_2$: C, 50.43; H, 6.57; N, 7.51. Found: C, 50.9; H, 6.7; N, 7.6.

**[$Zn_2$(L2-H)$PO_3$]$(ClO_4)_2$·3$H_2O$ (11).** [$Zn_2$(**L2**-H)]$(ClO_4)_3$·2$H_2O$ (37 mg, 0.04 mmol) and bis(*p*-nitrophenyl) phosphate (BNP) (34 mg, 0.1 mmol) were dissolved in water (20 $cm^3$), and the pH of the solution was adjusted to 10 by addition of 0.1 M NaOH. The resulting solution was kept at 35 °C for 5 days. The pH of the solution was periodically checked and kept constant at 10 by addition of small amounts of 0.1 M NaOH. The solution was then evaporated at 5 $cm^3$, and the pH was adjusted to 8 with 0.1 M $HClO_4$. $NaClO_4$ (50 mg) was then added. Evaporation of this solution led to the formation of a yellowish thick oil, which was collected and dissolved in a 1 M $NaClO_4$ aqueous solution. A yellowish solid was obtained by evaporation of this solution. This process was repeated twice to give a colorless powder. Yield: 10 mg (27%). Anal. Calcd for $C_{22}H_{55}Cl_2N_6O_{19}PZn_2$: C, 28.10; H, 5.90; N, 8.94; P, 3.29. Found: C, 28.0; H, 5.8; N, 8.9; P, 3.3. $^{31}$P NMR ($D_2O$, pH 10) (ppm): 7.8 (t, $J_{H-P}$ = 11.2 Hz).

**[$H_5$[(L2-H)$PO_3$]]$(ClO_4)_3$.** Compound **11** (10 mg, 0.11 mmol) was dissolved in water (3 $cm^3$), and the pH of the solution was adjusted to 3.5 with 0.1 mol $dm^3$ $HClO_4$. Addition of $NaClO_4$ (50 mg) led to precipitation of [$H_5$[(**L2**-H)$PO_3$]]$(ClO_4)_3$ as a white solid. Yield: 8 mg (84%). Anal. Calcd for $C_{22}H_{54}Cl_3N_6O_{20}P$: C, 30.76; H, 6.34; N, 9.79; P, 3.61. Found: C, 30.8; H, 6.4; N, 9.7; P, 3.4. $^1$H NMR ($D_2O$, pH 3.5) (ppm): 3.23 (t, 4H), 3.35 (t, 4H), 3.52 (m, 8H) (N−$CH_2$−$CH_2$−N ethylenic chains), 3.32 (m, 8H), 3.78 (m, 8H) (N−$CH_2$−$CH_2$−O), 3.68 (m, 8H) (O−$CH_2$−$CH_2$−O), 2.98 (t, 2H), 3.56 (t, 2H) (N−$CH_2$−$CH_2$−OH). $^{13}$C NMR ($D_2O$, pH 4) (ppm): 44.6, 44.7, 45.0, 50.5 (N−$CH_2$−$CH_2$−N ethylenic chains), 66.3, 66.2, 48.2, 49.8 (N−$CH_2$−$CH_2$−O ethylenic chains), 70.3, 70.6 (O−$CH_2$−$CH_2$−O ethylenic chain), 58.2, 60.0 (N−$CH_2$−$CH_2$−OH). $^{31}$P NMR ($D_2O$, pH 4) (ppm): 6.43 (t, $J_{H-P}$ = 9.8 Hz). MS (ESI) (*m*/*z*): 759 ([$H_5$[(**L2**-H)$PO_3$]]$(ClO_4)_2^+$), 379 ([[$H_5$[(**L2**-H)$PO_3$]]$(ClO_4)_3$]$HClO_4^{2+}$), 658 ([[$H_5$[(**L2**-H)$PO_3$]]$(ClO_4)_3$]-$(HClO_4)_2^+$).

**X-ray Structure Analysis.** A colorless prismatic crystal of [$Zn_2$-(**L**-H)$Br_2$]$BPh_4$·$CH_3OH$ was mounted on an Enraf NONIUS X-ray diffractometer, which uses an equatorial geometry. Graphite-monochromated Mo Kα radiation was used for cell parameter determination and data collection. A summary of the crystallographic data is reported in Table 1.

**Table 1.** Crystal Data and Structure Refinement Details for [$Zn_2$(**L2**-H)$Br_2$]$BPh_4$·MeOH

| | |
|---|---|
| empirical formula | $C_{47}H_{73}BBr_2N_6O_6Zn_2$ |
| formula weight | 1119.48 |
| temperature | 298 K |
| wavelength | 0.710 69 Å |
| crystal system | triclinic |
| space group | $P\bar{1}$ |
| unit cell dimensions | $a$ = 12.329(7) Å, α = 112.23(5)°, $b$ = 14.501(9) Å, β = 98.45(8)°, $c$ = 18.504(9) Å, γ = 101.13(9)° |
| volume | 2915(3) $Å^3$ |
| $Z$ | 2 |
| density (calcd) | 1.275 $Mg/m^3$ |
| absorption coefficient | 2.238 $mm^{-1}$ |
| crystal size | 0.25 × 0.2 × 0.1 mm |
| final $R$ indices [$I > 2\sigma(I)$] | R1 = 0.0822, wR2 = 0.2202[a] |
| $R$ indices (all data) | R1 = 0.1788, wR2 = 0.2805[a] |

[a] $R1 = \sum||F_o| - |F_c||/\sum|F_o|$; $wR2 = [\sum w(F_o^2 - F_c^2)^2/\sum wF_o^4]^{1/2}$.

Cell parameters were determined by least-squares refinement of diffractometer setting angles of 25 carefully centered reflections. The crystal of the compound belongs to the triclinc family, space group $P\bar{1}$, ($Z$ = 2), with $a$ = 12.329(7) Å, $b$ = 14.501(9) Å, $c$ = 18.504(9) Å, α = 112.23(5)°, β = 98.45(8)°, γ = 101.13(9)°, and $V$ = 2915(3) $Å^3$.

Intensities of two standard reflections were monitored during data collection to check the stability of the diffractometer and of the crystal: no loss of intensity was recognized. A total of 5571 reflections, up to 2-$\theta$ = 40°, were collected. Intensity data were corrected for Lorentz and polarization effects, and an absorption correction was

applied once the structure was solved by the Walker and Stuart method[39] (maximum/minimum corrections for $\mu$ and $\theta$ 1.341 596/0.753 641; maximum/minimum corrections for $\theta$ 1.129 545/0.956 054).

The structure was solved by the direct method of the SIR92[40] program. Refinements were performed by means of the full-matrix least-squares method of the SHELXL-93,[41] program which uses the analytical approximation for the atomic scattering factors and anomalous dispersion correction from ref 42. The function minimized was $\sum w(|F_o|^2 - |F_c|^2)^2$, with $w = 1/\sigma^2(F_o^2) + (aP)^2 + bP]$ where $a$ and $b$ are refined parameters and $P = F_o^2/3 + 2F_c^2/3$.

Disorder affects the ethylenic chains of the ligand and the tetraphenylborate anion: double positions were introduced in the calculation for the atoms C5 and C5′ (population parameters 0.7 and 0.3, respectively) and C15, C15′, C16, C16′, O4, and O4′ (population parameters 0.6 and 0.4 for the X and the X′, respectively). In addition, the FLAT and SIMU restraints of SHELXL-93[41] were used for atoms C42, C43, C44, C45, C46, and C47 belonging to a phenyl ring of a $BPh_4^-$ ion.

Anisotropic displacement parameters were used for all of the non-hydrogen atoms, except for those in double positions. The hydrogen atoms belonging to the macrocycle and to the $BPh_4^-$ ion were introduced in calculated positions, and their coordinates were refined in agreement with those of the linked atoms, with overall refined thermal parameters for the aliphatic and aromatic hydrogens, respectively. For 565 refined parameters, the final agreement factors were R1 = 0.0822 (for 2963 observed reflections with $I > 2.0\sigma(I)$) and wR2 = 0.2805.

**Emf Measurements.** All potentiometric measurements (pH = $-\log[H^+]$) were carried out at 298.1 ± 0.1 and 308.1 ± 0.1 K, by using the equipment which has been already described.[43] The reference electrode was an Ag/AgCl electrode in saturated KCl solution. The glass electrode was calibrated as a hydrogen concentration probe by titrating known amounts of HCl with $CO_2$-free NaOH solutions and determining the equivalent point by Gran's method,[44,45] which allows one to determine the standard potential $E°$ and the ionic product of water ($K_w = [H^+][OH^-]$). Titrations for the determination of the ligand basicity constants and Zn(II) complexation constants at 308.1 K were performed, in the pH range 2.5−10, by using $CO_2$-free aqueous solutions containing the ligand and or the metal ion in $1 \times 10^{-3}$−$2 \times 10^{-3}$ mol dm$^{-3}$ concentrations. The system Zn−**L2** was studied in 0.1 mol dm$^{-3}$ $NMe_4NO_3$ at 298.1 and 308.1 K (p$K_w$ = 13.83 and 13.40 at 298.1 and 308.1 K, respectively). At least three measurements were performed for each system (100 data points for each measurement). The computer program HYPERQUAD[46] was used to calculate both protonation and stability constants from emf data. The titration curves for each system were treated either as a single set or as independent entities without significant variations in the values of the stability constants.

**Kinetics of *p*-Nitrophenyl Acetate (NA) and Bis(*p*-nitrophenyl) Phosphate (BNP) Hydrolysis.** The hydrolysis rate of NA in the presence of the Zn−**L2** complexes was measured by an initial-slope method following the increase in the 403 nm absorption of the released *p*-nitrophenate at 298 ± 0.1 K by using the procedure reported in ref 34. The molar adsorbance of *p*-nitrophenate was determined at the pH of each measurement. The ionic strength was adjusted to 0.1 with $NMe_4NO_3$. MOPS (pH 7−7.8), TAPS (pH 7.8−8.9), and CHES (pH 8.9−9.5) buffers were used (50 mM). In a typical experiment, after NA and $[Zn_2(\mathbf{L2}\text{-H})](ClO_4)_3 \cdot 2H_2O$ (0.1−1 mM) in 10% $CH_3CN$ solution at appropriate pH (the reference experiment does not contain the Zn(II) complex) were mixed, the UV absorption decay was recorded immediately and was followed generally until 2% decay of NA. Two species, $[Zn_2(\mathbf{L2}\text{-H})]^{3+}$ and $[Zn_2(\mathbf{L2}\text{-H})(OH)]^{2+}$, promote NA hydrolysis; measurements in the pH range 6.8−7.5, where the $[Zn_2(\mathbf{L2}\text{-H})(OH)]^{2+}$ complex is absent from the solution, allow one to determine second-order $k_1$ constants for promoted hydrolysis by $[Zn_2(\mathbf{L2}\text{-H})]^{3+}$ and to extrapolate the $k_1$ values for this species in the pH range 7.5−9, where both species are present in solution. Measurements in the pH range 7.5−9 lead to the determination of $k_{obs}$ values. The second-order rate constants $k_2$ for $[Zn_2(\mathbf{L2}\text{-H})(OH)]^{2+}$ are calculated by subtracting from the $k_{obs}$ value at a given pH the $k_1$ value at the same pH. Errors in the final $k_{NA}$ values were about 10%.

The hydrolysis rate of BNP to give mono(*p*-nitrophenyl) phosphate and *p*-nitrophenate was measured in aqueous solution at 308 ± 0.1 K by using a method and procedure similar to those reported for NA hydrolysis. The visible absorption increase at 403 nm was recorded immediately after mixing BNP (1−10 mM) and $[Zn_2(\mathbf{L2}\text{-H})](ClO_4)_3 \cdot 2H_2O$ (1−10 mM) aqueous solutions and was followed generally until 0.2% formation of *p*-nitrophenate (for each second-order rate constant determination, at least five experiments were followed until 5−10%). A plot of the hydrolysis rate vs BNP concentration (1−10 mM) at a given pH gave a straight line, and then we determined the slope/[zinc complex] as the second-order rate constants $k_{BNP}$ ($M^{-1}$ $s^{-1}$). Errors in $k_{BNP}$ values were about 5%.

**Scheme 2**

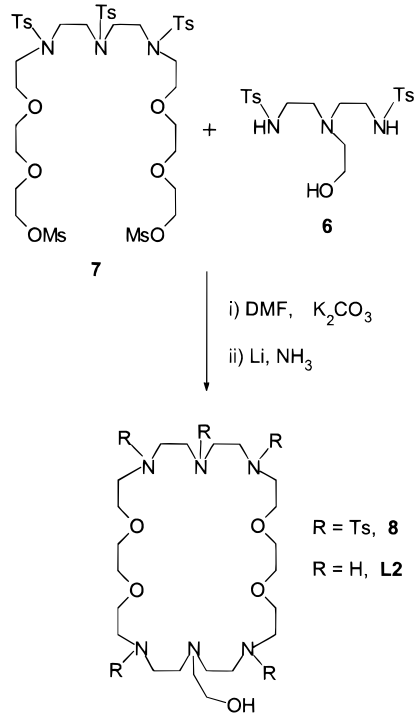


## Results and Discussion

**Synthesis.** The synthetic pathway used for the preparation of **L2** is depicted in Scheme 2. Reaction of tosylated amino alcohol **6** with the methylsulfonyl derivative **7**,[33,47] in DMF in the presence of $K_2CO_3$, a modification of the method of Richman and Atkins,[48] affords, after purification by chromatography, the tosylated macrocycle **8**. Removal of the protecting tosyl groups is the critical step of this route, due to the cleavage of ether linkage or oxidation of the alcoholic function by using acidic detosylation methods.[49] Although giving a low yield, this step was finally performed by employing Li in liquid $NH_3$.[50]

(39) Walker, N.; Stuart, D. D. *Acta Crystallogr., Sect. A* **1983**, *39*, 158−166.
(40) Altamore, A.; Cascarano, G.; Giacovazzo, C.; Guagliardi, A. *J. Appl. Crystallogr.* **1993**, *26*, 343.
(41) Sheldrick, G. M. *SHELXL-93*: *Program for Crystal Structure Refinement*; Institut für anorganische Chemie, Universität Göttingen: Göttingen, Germany, 1993.
(42) *International Tables for X-ray Crystallography*; Kynoch: Birmingham, England, 1974; Vol. IV.
(43) Bianchi, A.; Bologni, L.; Dapporto, P.; Micheloni, M.; Paoletti, P. *Inorg. Chem.* **1984**, *23*, 1201−1205.
(44) Gran, G. *Analyst* **1952**, *77*, 661−663.
(45) Rossotti, F. J.; Rossotti, H. *J. Chem. Educ.* **1965**, *42*, 375−378.
(46) Gans, P.; Sabatini, A.; Vacca, A. *Talanta* **1996**, *43*, 807−812.
(47) Qian, L.; Sun, Z.; Mertes, M. P.; Mertes, K. B. *J. Org. Chem.* **1991**, *56*, 4904−4907.
(48) Richman, J. E.; Atkins, T. J. *J. Am. Chem. Soc.* **1974**, *96*, 2268−2270.
(49) Bencini, A.; Bianchi, A.; Garcia-España, E.; Giusti, M.; Micheloni, M.; Paoletti, P. *Inorg. Chem.* **1987**, *26*, 681−684.

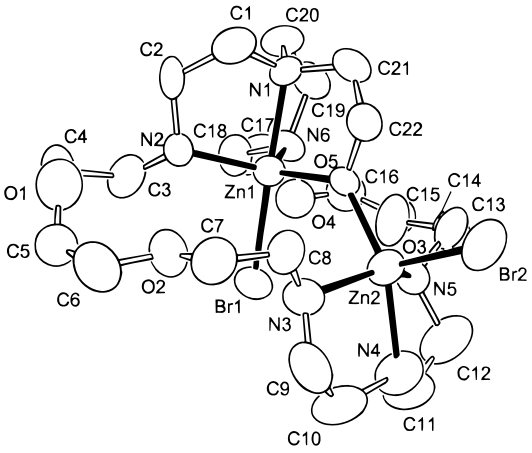


**Figure 1.** ORTEP drawing of the $[Zn_2(\mathbf{L2}\text{-H})Br_2]^+$ cation.

**Table 2.** Selected Bond Lengths (Å) and Angles (deg) for $[Zn_2(\mathbf{L2}\text{-H})Br_2]BPh_4\cdot MeOH$

| | | | |
|---|---|---|---|
| Zn1−O5 | 1.985(10) | Zn2−O5 | 2.019(11) |
| Zn1−N6 | 2.089(14) | Zn2−N5 | 2.120(14) |
| Zn1−N2 | 2.115(14) | Zn2−N3 | 2.13(2) |
| Zn1−N1 | 2.175(14) | Zn2−N4 | 2.18(2) |
| Zn1−Br1 | 2.507(4) | Zn2−Br2 | 2.416(4) |
| O5−Zn1−N6 | 117.4(5) | O5−Zn2−N5 | 91.9(5) |
| O5−Zn1−N2 | 119.7(5) | O5−Zn2−N3 | 92.0(5) |
| N6−Zn1−N2 | 117.9(6) | N5−Zn2−N3 | 138.9(6) |
| O5−Zn1−N1 | 82.6(5) | O5−Zn2−N4 | 156.7(6) |
| N6−Zn1−N1 | 82.5(6) | N5−Zn2−N4 | 80.3(6) |
| N2−Zn1−N1 | 82.5(6) | N3−Zn2−N4 | 80.2(7) |
| O5−Zn1−Br1 | 96.5(3) | O5−Zn2−Br2 | 106.0(3) |
| N6−Zn1−Br1 | 96.8(4) | N5−Zn2−Br2 | 109.5(4) |
| N2−Zn1−Br1 | 99.1(4) | N3−Zn2−Br2 | 108.6(4) |
| N1−Zn1−Br1 | 178.4(4) | N4−Zn2−Br2 | 97.3(5) |

**Crystal Structure of $[Zn_2(L2\text{-H})Br_2]BPh_4\cdot MeOH$.** The molecular structure consists of $[Zn_2(\mathbf{L2}\text{-H})Br_2]^+$ binuclear complex cations, tetraphenylborate anions, and disordered methanol molecules. An ORTEP[51] drawing of the $[Zn_2(\mathbf{L2}\text{-H})Br_2]^+$ cation is shown in Figure 1, and Table 2 reports selected distances and angles for the metal coordination environment.

Each metal atom is bound by a triaza moiety, with the deprotonated alcoholic pendant bridging almost symmetrically the two metal ions (Zn1−O5 = 1.985(10) Å, Zn2−O5 = 2.019(11) Å), with a Zn1−O5−Zn2 angle of 124.8(6)°. The two metals lie 3.549(5) Å apart from each other. The coordination sphere of each metal is completed by a bromide ion, resulting in a five-coordinated environment. The Zn1 atom is coordinated by N1, N2, N6, O5, and Br1 in an almost regular bipyramidal arrangement. The axial positions are occupied by the tertiary nitrogen N1 and by Br1, while N2, N6, and O5 occupy the equatorial positions. The Zn2 atom is coordinated by N3, N4, N5, O5, and the Br2 bromide. The coordination geometry is remarkably different from that of Zn1 and can be best described as a distorted square pyramid. The basal plane is defined by O5, N3, N4, and N5 (maximum deviation from the mean plane 0.23(2) Å for N4). The Zn2 atom lies 0.563(3) Å from this plane, shifted toward the apical position, which is occupied by Br2.

It is of interest to compare the present structure with that of the **L1** dizinc complex $[Zn_2(\mu\text{-OH})\mathbf{L1}]^{3+}$.[33] In this complex the coordination geometries of the metals are almost equal: each Zn(II) is coordinated by a triamine moiety, two ethereal oxygens, and a bridging hydroxide anion, with a Zn···Zn distance of 3.543 Å. In $[Zn_2(\mu\text{-OH})\mathbf{L1}]^{3+}$, the macrocycle assumes a screw-shaped conformation, defining a tridimensional internal cavity where the $Zn_2(\mu\text{-OH})$ unit is deeply encapsulated. In $[Zn_2(\mathbf{L2}\text{-H})Br_2]^+$, the Zn···Zn distance is almost equal (3.549(5) Å), but the Zn1−O−Zn2 angle is remarkably smaller than that in $[Zn_2(\mu\text{-OH})\mathbf{L1}]^{3+}$ (124.8 vs 137.4°). Furthermore, in $[Zn_2(\mathbf{L2}\text{-H})Br_2]^+$, the macrocyclic ligand adopts an overall chair conformation, more "opened" than that in $[Zn_2(\mu\text{-OH})\mathbf{L1}]^{3+}$. Therefore, the $Zn_2(\mu\text{-RO})$ function is less crowded and shielded than the $Zn_2(\mu\text{-OH})$ function. Finally, although in $[Zn_2(\mathbf{L2}\text{-H})Br_2]^+$ both metals have the same set of donors, it should be noted that Zn1 is almost embedded inside a tridimensional cavity defined by the triamine moiety N1−N2−N6 and by the alcoholic pendant. The other metal ion (Zn2), located in the N3−N4−N5 moiety, is less shielded by the macrocyclic framework.

Enzymes able to cleave phosphate ester bonds often contain carboxylate-bridged dimetallic cores, with consequent short intermetallic separations. A recent crystal structure of native *Escherichia coli* alkaline phosphatase complexed with inorganic phosphate shows the phosphate anion bridging the two Zn(II) ions, which lie 3.94 Å apart from each other.[10−13] A shorter Zn···Zn distance is achieved in our complex. It is to be noted, however, that such a short separation is due not only to the inclusion of two metals within a cyclic framework but also to the bridging alkoxide, which forces the two Zn(II) ions close to each other.

**Table 3.** Logarithms of the Equilibrium Constants for the Complexation Reactions of Zn(II) with **L1** and **L2**

| | log *K* | | | |
|---|---|---|---|---|
| | **L1** | | **L2** | |
| reaction | 298.1 K | 308.1 K[a] | 298.1 K | 308.1 K |
| $Zn^{2+} + \mathbf{L} = Zn\mathbf{L}^{2+}$ | 8.31(7) | 8.0 | 9.55(4) | 9.36(8) |
| $Zn\mathbf{L}^{2+} + H^+ = ZnH\mathbf{L}^{3+}$ | 8.16(7) | 8.4 | 8.01(5) | 7.68(7) |
| $ZnH\mathbf{L}^{3+} + H^+ = ZnH_2\mathbf{L}^{4+}$ | 7.11(5) | 6.7 | 7.10(3) | 6.62(8) |
| $pK_a$[b] | 9.6(1) | | 9.27(4) | 8.9(1) |
| $Zn\mathbf{L}^{2+} + Zn^{2+} = Zn_2\mathbf{L}^{4+}$ | 5.02(5) | 5.4 | 4.85(3) | 3.7(1) |
| $pK_{a1}$[c] | 7.08(4) | 7.01 | 6.92(3) | 5.94(5) |
| $pK_{a2}$[d] | 8.64(6) | 9.1 | 8.46 | 7.92 |

[a] From ref 33. [b] $K_a$ is relative to the equilibria $Zn\mathbf{L}^{2+} + H_2O = Zn\mathbf{L}OH^+ + H^+$. [c] $K_{a1}$ is relative to the equilibria $Zn_2\mathbf{L}^{4+} + H_2O = Zn_2\mathbf{L}(OH)^{3+} + H^+$ for $\mathbf{L} = \mathbf{L1}$ and $Zn_2\mathbf{L}^{4+} = Zn_2(\mathbf{L}\text{-H})^{3+} + H^+$ for $\mathbf{L} = \mathbf{L2}$. [d] $K_{a2}$ is relative to the equilibria $Zn_2\mathbf{L}(OH)^{3+} + H_2O = Zn_2\mathbf{L}(OH)_2^{2+} + H^+$ for $\mathbf{L} = \mathbf{L1}$ and $Zn_2(\mathbf{L}\text{-H})^{3+} + H_2O = Zn_2(\mathbf{L}\text{-H})(OH)^{2+} + H^+$ for $\mathbf{L} = \mathbf{L2}$.

**Zn(II) Complexation in Aqueous Solution.** Ligand protonation[52] and Zn(II) coordination by **L2** were studied by means of potentiometric titrations in 0.1 mol $dm^{-3}$ $NMe_4NO_3$ at 298.1 and 308.1 K. Table 3 summarizes the obtained formation constants of the Zn(II) complexes with **L2**, in comparison with the previously reported constants of **L1**.[33] **L2** forms mono- and dinuclear complexes in aqueous solutions. As shown in Table 3, the mononuclear $[Zn\mathbf{L2}]^{2+}$ complex displays a stability similar to that found for triamine ligands, such as 1,4,7-triazaheptane (log *K* = 8.9),[53] and a high tendency to protonate (the two first

(50) Lehn, J. M.; Montavon, F. *Helv. Chim. Acta* **1976**, *59*, 1566−1582.
(51) Johnson, C. K. *ORTEP*; Report ORNL-3794; Oak Ridge National Laboratory: Oak Ridge, TN, 1971.
(52) Protonation constants of **L2** at 298.1 K: log $K_1$ = 9.84(2), log $K_2$ = 8.89(2), log $K_3$ = 8.32(2), log $K_4$ = 7.61(2), log $K_5$ = 3.84(2), log $K_6$ = 1.95(3) (0.1 mol $dm^{-3}$ $NMe_4NO_3$ aqueous solution, 298.1 K); log $K_1$ = 9.44(2), log $K_2$ = 8.51(2), log $K_3$ = 8.01(2), log $K_4$ = 7.04(2), log $K_5$ = 3.51(4), log $K_6$ = 1.65(9) (0.1 mol $dm^{-3}$ $NMe_4NO_3$ aqueous solution, 308.1 K).
(53) Smith, R. M.; Martell, A. E. *Critical Stability Constants;* Plenum Press: New York, 1975; Vol. 2. See also 1st supplement, 1982.

protonation constants are only 1.2−1.3 log units lower than the corresponding basicity constants of the free amine), suggesting that protonation of the $[Zn\mathbf{L2}]^{2+}$ complex takes place on nitrogen atoms not bound to the metal cation. These observations indicate that the metal ion is coordinated by one of the two triamine moieties, while the other one does not participate in the coordination. The fact that the $[Zn\mathbf{L2}]^{2+}$ complex shows a somewhat higher stability than $[Zn\mathbf{L1}]^{2+}$ (log $K$ = 9.55 for $[Zn\mathbf{L2}]^{2+}$ vs log $K$ = 8.31 for $[Zn\mathbf{L1}]^{2+}$) may indicate that, in the **L2** complex, the Zn(II) ion is coordinated by the triamine unit bearing the alcoholic function, which could act as a further binding site for the metal ion.

The mononuclear $[Zn\mathbf{L2}]^{2+}$ complex shows a marked tendency to bind a second metal, giving binuclear complexes. Binuclear complexes are largely prevalent in aqueous solution containing the ligand and Zn(II) in a 1:2 molar ratio (Figure S1, Supporting Information). The formation of the binuclear $[Zn_2\mathbf{L2}]^{4+}$ complex takes place at pH >6, with almost simultaneous deprotonation of the pendant alcoholic OH to give the $[Zn_2(\mathbf{L2}\text{-H})]^{3+}$ complex. Deprotonation of the alcohol group is confirmed by the analysis of the $^1$H NMR spectra of the complex recorded at different pH values. In fact, the resonance of the protons of the methylenic group in the α-position with respect to the OH function (a multiplet at $\delta$ = 3.74 ppm) exhibits a marked upfield shift in the pH range 6.5−8 (0.3 ppm), where the formation of $[Zn_2(\mathbf{L2}\text{-H})]^{3+}$ takes place, suggesting deprotonation of OH and simultaneous binding to the two metal centers.

The most significant finding is the extremely facile deprotonation of the alcoholic function with p$K_{a1}$ values (Table 3) of 6.92 (at 298.1 K) and 5.94 (at 308.1 K). It is of interest to note that these p$K_a$ values are lower than those found by Kimura et al. for the mononuclear Zn(II) complexes **1** and **2** (p$K_a$ = 7.4 and 7.60, respectively, at 298.1 K),[28,29] where deprotonation of the alcoholic function is assisted by a single metal ion. It can be concluded that the low p$K_a$ value of the present dizinc complex is due to the bridging coordination of the alkoxide function to the two metal centers, as actually shown by the crystal structure of the $[Zn_2(\mathbf{L2}\text{-H})Br_2]^+$ cation. In $[Zn_2(\mathbf{L2}\text{-H})Br_2]^+$, each metal is coordinated by a triamine moiety, the bridging alkoxide, and two bromide anions. Most likely, the bromide anions are replaced by water molecules in aqueous solution, which may deprotonate, giving hydroxo complexes. Actually, the formation of a monohydroxo $[Zn_2(\mathbf{L2}\text{-H})(OH)]^{2+}$ complex is observed at alkaline pH's (Figure S1), with p$K_{a2}$ values of 8.46 (298.1 K) and 7.92 (308.1 K). These p$K_a$ values are higher than those usually found for bridging hydroxide groups.[33,34] For instance, in the dinuclear Zn(II) complex with ligand **L1**, a water molecule deprotonates to give the hydroxide-bridged $[[Zn_2(\mu\text{-OH})\mathbf{L1}]^{3+}$ complex with a p$K_{a1}$ value of 7.09 (0.1 mol dm$^{-3}$ $NMe_4NO_3$, 298.1 K). This suggests that, in $[Zn_2(\mathbf{L2}\text{-H})(OH)]^{2+}$, the hydroxide anion binds to a single metal. Considering the crystal structure of $[Zn_2(\mathbf{L2}\text{-H})Br_2]^+$, hydroxide would bind to Zn2, less shielded by the macrocyclic framework than Zn1. Hydroxide binding also affects the binding mode of the alkoxide group. The $^1$H signal of the $CH_2$ group in the α-position with respect to the alkoxide function shifts 0.2 ppm upfield in the pH range 8.5−9.5, where the formation of $[Zn_2(\mathbf{L2}\text{-H})(OH)]^{2+}$ occurs. Most likely, the addition of a strongly bound hydroxide to a Zn(II) ion leads to detachment of the alkoxide function from one of the metals or to a weakening of a Zn(II)−OR bond, as sketched in Chart 1.

These characteristics make the dinuclear zinc complex with **L2** a promising model for AP, where both a deprotonated hydroxyl group and a Zn−OH function act as nucleophiles in the hydrolytic process. In the present complex, Zn(II)-assisted deprotonation of the alcohol pendant takes place at neutral or slight alkaline pH. Besides that, further deprotonation of a water molecule gives the $[Zn_2(\mathbf{L2}\text{-H})(OH)]^{2+}$ complex, which contains both the R−O$^-$−Zn(II) and Zn(II)−OH nucleophilic functions. Although several complexes containing an R−O$^-$−Zn(II) or a Zn(II)−OH function have been synthesized to elucidate their roles in hydrolytic processes,[15−34] this is the first complex containing both a Zn(II)-bound alkoxide and a Zn(II)-bound hydroxide at close distance, which may act cooperatively in carboxy or phosphate ester cleavage.

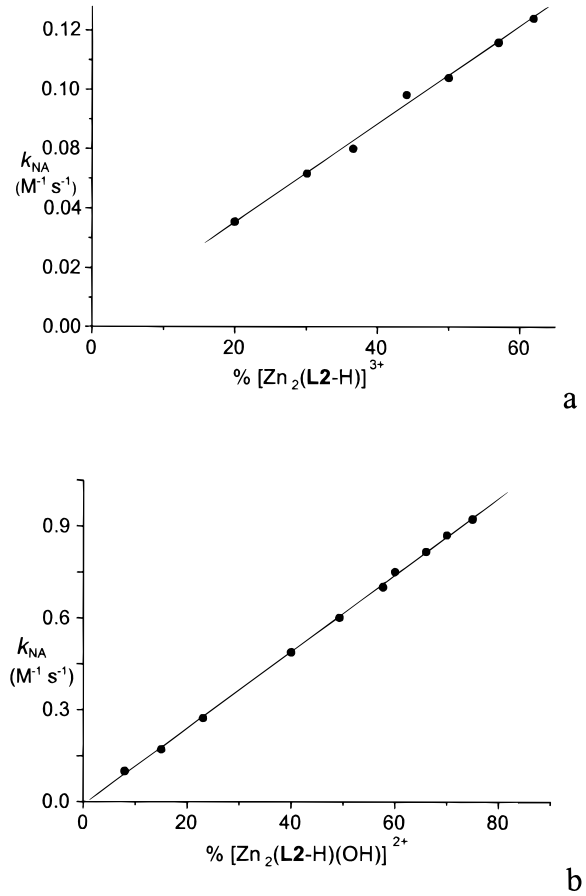


**Figure 2.** Second-order rate constants for NA hydrolysis ($k_{NA}$) as a function of the percentage of the complexes $[Zn_2(\mathbf{L2}\text{-H})]^{3+}$ (a) and $[Zn_2(\mathbf{L2}\text{-H})(OH)]^{2+}$ (b) determined in 0.1 mol dm$^{-3}$ $NMe_4NO_3$ aqueous solution at 298 K.

To test the hydrolytic activity of this system, we undertook a study of activated carboxy and phosphate ester hydrolysis promoted by the dizinc **L2** complex.

***p*-Nitrophenyl Acetate (NA) Hydrolysis.** Both the dinuclear complexes $[Zn_2(\mathbf{L2}\text{-H})]^{3+}$ and $[Zn_2(\mathbf{L2}\text{-H})OH]^{2+}$ promote NA hydrolysis at 298 K, and second-order kinetics are followed at different pH values. In Figure 2, the $k_{NA}$ values are reported as a function of the percentages of the $[Zn_2(\mathbf{L2}\text{-H})]^{3+}$ and $[Zn_2(\mathbf{L2}\text{-H})OH]^{2+}$ complexes. No effect is observed below pH 6.5, where such species are absent in solutions. In both cases, the plots give rise to straight lines. These results indicate that the deprotonated complexes $[Zn_2(\mathbf{L2}\text{-H})]^{3+}$ and $[Zn_2(\mathbf{L2}\text{-H})OH]^{2+}$ are the kinetically active species. NA hydrolysis was also followed by recording $^1$H NMR spectra of aqueous solutions containing NA and the dizinc complex in the pH range 7−9. The NMR data account for the formation of a transient acetyl

**Scheme 3**

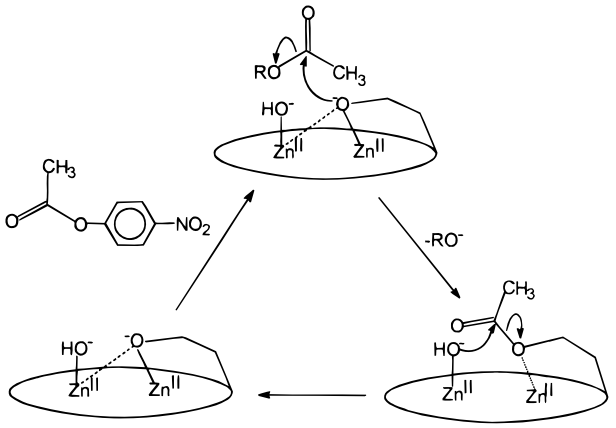


**9**

intermediate (**9** in Scheme 3), which is rapidly hydrolyzed to give acetate.

For instance, the $^1$H NMR spectrum recorded at pH 7.5 (Tris buffer, 298 K) ca. 5 min after mixing $[Zn_2(\mathbf{L2}\text{-H})](ClO_4)_3\cdot 2H_2O$ and NA (both $2 \times 10^{-3}$ mol dm$^{-3}$) shows the formation of free *p*-nitrophenate (two doublets at 6.72 and 8.28 ppm), accompanied by the appearance of a sharp singlet at 2.36 ppm, which can be reasonably assigned to the methyl group of transient **9**, together with the signal of the methyl group of acetate at 2.14 ppm. The signal of the methyl group of **9** completely disappears in about 1 h to give the spectrum of acetate and the starting dizinc complex. The rate of decomposition of **9** is strongly pH dependent: it becomes faster at alkaline pH, being too fast at pH >8 (298 K) to allow the observation of the intermediate in the $^1$H NMR spectra at 298 K. Anyway, $^1$H NMR spectra recorded at lower temperatures (278 K) allow one to observe intermediate **9** up to pH 8.5. On this basis, we propose the overall catalytic reaction depicted in Scheme 3, in which the slowest step is the initial formation of the acetyl intermediate **9**. The formation of a similar intermediate was also observed by Kimura et al. in NA hydrolysis catalyzed by the mononuclear Zn(II) complexes **1** and **2**.[28,29] **9** is subsequently hydrolyzed through an intramolecular nucleophilic attack of a coordinated water molecule at neutral pH or by a more strongly nucleophile Zn−OH function generated at alkaline pH's. It is to be noted that, as in AP, both the nucleophilic R−O$^-$−Zn and Zn−OH functions are involved in this hydrolytic process.

The $[Zn_2(\mathbf{L2}\text{-H})]^{3+}$ and $[Zn_2(\mathbf{L2}\text{-H})OH]^{2+}$ complexes are formed in at most 70% percentages in the pH ranges used in the kinetic measurements. As a consequence, to compare the activity of **L2** complexes with that of the **L1** ones, second-order rate constants $k'_{NA}$ were determined from the maximum $k_{NA}$ values by using the equation

$$v = k_{NA}[\text{total Zn(II) complex}][NA] = k'_{NA}[Zn_2(\mathbf{L2}\text{-H})^{3+}][NA]$$

The $k'_{NA}$ values for the present complex are reported in Table 4, together with the rate constants found for the binuclear complexes with **L1** and for the mononuclear Zn(II) complexes **1** and **2**. For the $[Zn_2\mathbf{L1}(OH)]^{3+}$ and $[Zn_2\mathbf{L1}(OH)_2]^{2+}$, complexes it was found that NA hydrolysis occurs via a simple bimolecular mechanism, which involves the nucleophilic attack of the metal-bound hydroxide on the carbonyl group of the ester. Furthermore, in $[Zn_2\mathbf{L1}(OH)]^{3+}$, the hydroxide anion bridges the two metals,[33] in a fashion similar to that found for the alkoxide group in $[Zn_2(\mathbf{L2}\text{-H})]^{3+}$. Comparing the kinetic data for both the R−O$^-$−Zn(II) and Zn(II)−OH reactive functions, we can conclude that a Zn(II)-bound alkoxide is a better nucleophile than a Zn(II)-bound hydroxide. For instance, the bridging alkoxide in $[Zn_2(\mathbf{L2}\text{-H})]^{3+}$ is ca. twice more active than the bridging hydroxide in $[Zn_2\mathbf{L1}(OH)]^{3+}$. The observation that the alkoxide function is a stronger nucleophile than a hydroxide function is in good accord with the results previously found by Kimura et al. in the case of mononuclear Zn(II) complexes.[28−31] However, the data in Table 4 also show that the $[Zn_2(\mathbf{L2}\text{-H})]^{3+}$ complex exhibits nucleophilic activity similar to that of complex **1**[28] but lower than complex **2**,[29] suggesting that a bridging RO$^-$ function is less nucleophilic than a single-coordinated R−O$^-$−Zn(II) group. This is not surprising, considering that a bridging coordination of alkoxide to two electrophilic metal centers may reduce the nucleophilic character of this group. In contrast, the hydroxo complex $[Zn_2(\mathbf{L2}\text{-H})OH]^{3+}$ is much more active than $[Zn_2(\mathbf{L2}\text{-H})]^{3+}$; i.e., binding of hydroxide increases the nucleophilicity of the R−O$^-$ group. As previously discussed, this can be reasonably ascribed to the strong binding of a hydroxide anion to a single Zn(II) ion, which leads to a partial detachment of the deprotonated alcoholic function from the metal.

**Table 4.** Second-Order Rate Constants $k'_{NA}$ ($M^{-1}$ $s^{-1}$) for Hydrolysis of *p*-Nitrophenyl Acetate at 298 K

| nucleophile | $k'_{NA}$ ($M^{-1}$ $s^{-1}$) | nucleophile | $k'_{NA}$ ($M^{-1}$ $s^{-1}$) |
|---|---|---|---|
| $[Zn_2(\mathbf{L2}\text{-H})]^{3+}$ | $0.21 \pm 0.02$ | $[Zn_2\mathbf{L1}(OH)_2]^{2+}$ [a] | 1.3 |
| $[Zn_2(\mathbf{L2}\text{-H})(OH)]^{2+}$ | $1.6 \pm 0.1$ | **1** [b] | 0.14 |
| $[Zn_2\mathbf{L1}(OH)]^{3+}$ [a] | 0.094 | **2** [c] | 0.46 |

[a] From ref 34. [b] From ref 28. [c] From ref 29.

***p*-Nitrophenyl Phosphate (BNP) Cleavage.** The reaction of BNP with $[Zn_2(\mathbf{L2}\text{-H})](ClO_4)_3\cdot 2H_2O$ was followed by recording $^1$H and $^{31}$P spectra of aqueous solutions containing the anionic substrate and the complex (1:1 molar ratio, 318 K, 0.1 mol dm$^{-3}$ $NMe_4NO_3$). It is to be anticipated that the $[Zn_2(\mathbf{L2}\text{-H})]^{3+}$ complex does not promote this hydrolytic process. At pH 10 (CAPS buffer), ca. 1 h after mixing $[Zn_2(\mathbf{L2}\text{-H})](ClO_4)_3\cdot 2H_2O$ and BNP, a triplet ($J_{H-P} = 9.5$ Hz) at 7.3 ppm appears in the $^{31}$P spectrum. The time evolution of the $^{31}$P spectra shows an initial increase of intensity of this signal and a simultaneous decrease of that of BNP at −8.2 ppm (Figure S2, Supporting Information). The triplet at 7.3 ppm is attributed to the phosphoryl derivative **10** formed from the nucleophilic attack of the alkoxide function on phosphorus and release of *p*-nitrophenate (see Scheme 4). The same reaction was also followed by $^1$H NMR spectroscopy, and the product **10** was identified by two doublets of the aromatic moiety at 7.20 and 8.18 ppm.

The final product **11** appears subsequently, identified by a triplet in the $^{31}$P NMR spectra at 7.8 ppm ($J_{H-P} = 11.2$ Hz). This signal can be unambiguously assigned to the phosphate pendant complex **11** (see below). After 150 h, more than 90% of the initial dizinc complex **5** was converted to **11** and almost 2 equiv of *p*-nitrophenate was released. No other different mechanism or side product, even for low percentages of released *p*-nitrophenate, were detected by $^1$H and $^{31}$P NMR spectroscopy. Most likely, the hydrolytic process **10** → **11** takes place through an intramolecular attack of a Zn−OH function on the phosphorus, as previously observed for several Zn−OH species.[28−31,54,55]

(54) Jones, D. R.; Lindoy, L. F.; Sargeson, A. M. *J. Am. Chem. Soc.* **1983**, *105*, 7327−7336.
(55) Jones, D. R.; Lindoy, L. F.; Sargeson, A. M. *J. Am. Chem. Soc.* **1984**, *106*, 7807−7819.

**Scheme 4**

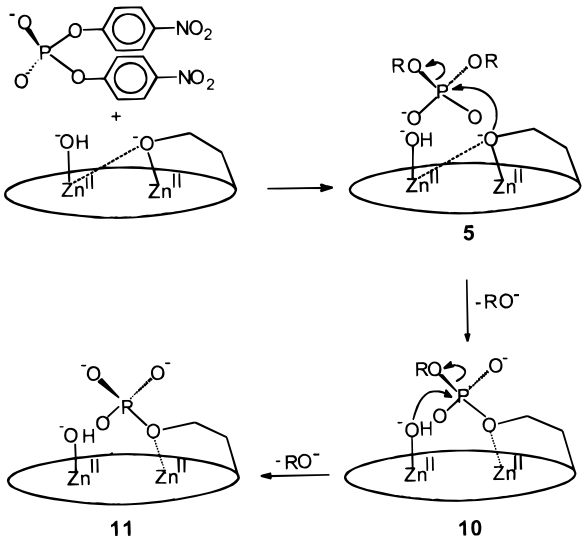


The phosphate pendant derivative **11** was isolated as a unique product from BNP cleavage (see Experimental Section). Zn(II) was then removed from the complex by treatment with diluted $HClO_4$, to give the metal-free pentaprotonated phosphoryl derivative $[H_5[(\mathbf{L2}\text{-H})PO_3]]^{3+}$, which was isolated as its perchlorate salt and fully characterized. Compound **11** is extremely inert and does not undergo further hydrolysis. A prolonged (ca. 2 week) reaction at 308 K (aqueous solution, pH 10) did not change the $^{31}P$ spectrum of **11**.

The initial phosphorylation rate of **5** → **10** was further studied by following the increase of the released *p*-nitrophenate at 308 K. The dinuclear $[Zn_2(\mathbf{L2}\text{-H})(OH)]^{2+}$ complex promotes BNP cleavage in aqueous solution at 308 K, and second-order rate constants $k_{BNP}$ have been determined at different pH values. In Figure 3 the $k_{BNP}$ values for the Zn−**L2** complexes are reported as a function of pH, together with the distribution curve of the $[Zn_2(\mathbf{L2}\text{-H})(OH)]^{2+}$ species at 308 K. A good fitting between the $k_{BNP}$ values and the distribution curve of the $[Zn_2(\mathbf{L2}\text{-H})(OH)]^{2+}$ species is found. Accordingly, it can be concluded that this complex is a kinetically active species. On the contrary, the $[Zn_2(\mathbf{L2}\text{-H})]^{3+}$ complex does not promote this hydrolytic process, in accord with the low nucleophilic character evidenced by this species in NA hydrolysis.

As in the case of NA hydrolysis, a second-order rate constant $k'_{BNP}$ of $(8.3 \pm 0.4) \times 10^{-4}$ can been determined from the maximum $k_{BNP}$ values. Once more, the $[Zn_2(\mathbf{L2}\text{-H})(OH)]^{2+}$ complex is more active (ca. 7 times) in BNP hydrolysis than the **L1** complex $[Zn_2\mathbf{L1}(OH)_2]^{2+}$ ($k'_{BNP} = 1.15 \times 10^{-4}$), where a Zn−OH function acts as a nucleophile in the hydrolytic mechanism. This result indicates that a $RO^-$−Zn(II) function acts as a better nucleophile than a Zn(II)−OH function also toward the phosphate ester. However, it should be observed that the reaction of BNP with $[Zn_2(\mathbf{L2}\text{-H})(OH)]^{2+}$ is a phosphoryl transfer to give the phosphoryl intermediate **10**, while the reaction of BNP with $[Zn_2\mathbf{L1}(OH)_2]^{2+}$ is a hydrolytic process that yields mono(nitrophenyl) phosphate.

## Concluding Remarks

The new alcohol-pendant macrocycle **L2** is a ditopic ligand for Zn(II); i.e., it contains two different binding sites (two triamine moieties, one of them bearing an ethanol pendant) for this metal. Therefore, it can form a stable dizinc complex from neutral to alkaline aqueous solutions. The alcoholic group deprotonates with $pK_a$ value of 6.9 at 298 K, to bridge both Zn(II) ions at the fourth coordination site. The resulting $[Zn_2(\mathbf{L2}\text{-H})]^{3+}$ complex, however, does not show a strong nucleophilic character in carboxy and phosphate ester hydrolysis, due to the bridging coordination to two electrophilic centers of the alkoxide function. At slightly alkaline pH's, a Zn(II)-coordinated water molecule undergoes hydrolysis ($pK_a = 8.46$ at 298.1 K), giving the $[Zn_2(\mathbf{L2}\text{-H})(OH)]^{2+}$ complex. This complex is the first system containing both a Zn(II)-bound alkoxide and a Zn−OH nucleophilic function, kept at close distance by the macrocyclic framework. Therefore, our complex may provide a simple model system for alkaline phosphatases, in which both a deprotonated serine and a Zn−OH group are involved in the hydrolysis of phosphate monoesters. Indeed, the $[Zn_2(\mathbf{L2}\text{-H})(OH)]^{2+}$ complex promotes BNP cleavage with rate constants much higher than those of the dizinc complex $[Zn_2\mathbf{L1}(OH)_2]^{2+}$, which contains two nucleophilic Zn−OH functions. Such a higher activity is due to the Zn(II)-bound alkoxide anion, a better nucleophile than the Zn(II)-bound hydroxide anion. Similar to the case of alkaline phosphatases, both the R−$O^-$−Zn(II) and Zn−OH nucleophilic functions are involved in the hydrolytic mechanism. The R−$O^-$−Zn(II) function acts as nucleophile in the first step of NA and BNP cleavage, giving an acetyl or a phosphoryl intermediate, which is subsequently hydrolyzed via an intramolecular attack of a Zn(II)−OH function.

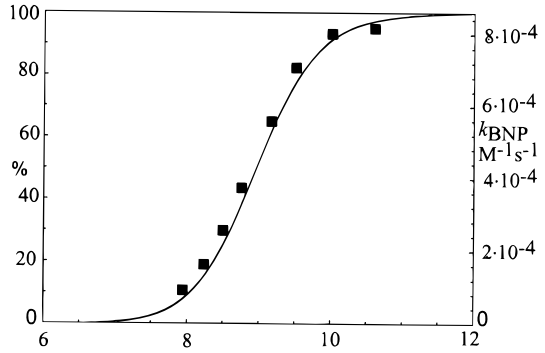


**Figure 3.** Plot of the distribution curve of $[Zn_2(\mathbf{L2}\text{-H})(OH)]^{2+}$ (solid line, right *y* axis) and $k_{BNP}$ values (■, left *y* axis) as a function of pH (0.1 mol $dm^{-3}$ $NMe_4NO_3$, 308 K).

**Acknowledgment.** Financial support from the Italian Ministero dell'Università e della Ricerca Scientifica e Tecnologica (quota 40%) and the CNR (Consiglio Nazionale delle Ricerche) is gratefully acknowledged. We wish to thank Dr. P. Rossi and Prof. P. Dapporto for their ongoing interest and support.

**Supporting Information Available:** An X-ray crystallographic file in CIF format, tables listing detailed crystallographic data, atomic positional parameters, anisotropic temperature factors, and bond distances and angles for $[Zn_2(\mathbf{L2}\text{-H})Br_2]BPh_4 \cdot MeOH$, a table of weighted least-squares planes, a table listing molar absorbance values of *p*-nitrophenate at different pH's, a distribution diagram for the system Zn(II)−**L2** (2:1 molar ratio), and a figure showing the time course of the percentages of BNP, **10**, and **11** for the reaction of BNP with $[Zn_2(\mathbf{L2}\text{-H})](ClO_4)_3 \cdot 2H_2O$. This material is available free of charge via the Internet at http://pubs.acs.org.

IC9902929